Solvatochromic Characterization of the Liquid Phase in Liquid–Supercritical CO_2 Mixtures

Sean P. Kelley and Richard M. Lemert
Chemical Engineering Dept., University of Toledo, Toledo, OH 43606

The solvatochromic dye phenol blue (N,N-dimethylindoaniline) is used to characterize the solvent strength (polarity) of the saturated liquid phase in a series of solvent–carbon dioxide binary mixtures. Data were obtained at 35 and 55°C and at pressures up to ~70 bar. Five solvents were investigated—acetone, cyclohexane, methanol, THF, and toluene. The polarity of the liquid phase decreases significantly with increasing pressure due to the increasing carbon dioxide content of this phase at equilibrium. For example, the polarity of acetone saturated with carbon dioxide at 35°C and ~60 bar is equivalent to the polarity of pure cyclohexane at ambient pressure. The local environment about the dye is significantly richer in the polar liquid component than the bulk composition would indicate. The degree of enrichment reflects concentration effects at low pressure, and both concentration and pressure effects at high pressure where the mixtures are highly compressible. The NRTL model of Renon and Prausnitz is able to predict these local compositions with reasonable accuracy except at CO_2-rich conditions where compressibility effects are important.

Introduction

The last fifteen years have seen a tremendous growth in the field of supercritical fluid technology. Most of the interest in this technology, however, has focused on its use as a solvent (McHugh and Krurkonis, 1994; Brennecke and Eckert, 1989; Savage et al., 1995; Kiran and Levelt Sengers, 1994). Carbon dioxide has played a particularly important role in this development due to its nontoxicity, nonflammability, and easily accessible critical point ($T_c = 304.4$ K; $P_c = 73.8$ bar). Pure carbon dioxide is a fairly weak solvent, however, with very little affinity for solutes with any appreciable polarity (Lemert and Johnston, 1991; Krukonis and Kurnik, 1985; Stahl, 1977; Stahl et al., 1982; Gurdial and Foster, 1991). As a result, a great deal of effort has gone into developing ways to enhance the solubilities of these polar compounds through such devices as the use of cosolvents (Brennecke and Eckert, 1989; Dobbs et al., 1987; Lemert and Johnston, 1991) and microemulsions (Harrison et al., 1994; Gupta et al., 1994; Newman et al., 1993).

In recent years it has been recognized that supercritical carbon dioxide, in addition to being an interesting and useful solvent, is also an important and effective *anti*solvent. Two different antisolvent processes have been developed. In the gas antisolvent (GAS) process, a solute is dissolved in an ordinary liquid, and this liquid phase is exposed to a supercritical fluid phase at moderate pressures. The fluid component dissolves in the liquid, expanding it and decreasing its solvent strength (i.e., cohesive energy density). Eventually the liquid phase is no longer able to support the solute and it drops out of solution. The liquid phase is present throughout the process, however. In the precipitation with a compressed antisolvent (PCA) process, on the other hand, the liquid solution is sprayed into the fluid phase through a nozzle. The solvent rapidly expands as it absorbs the fluid component, and at the same time it also dissolves in the fluid phase. The solutes dissolved in the liquid phase are not soluble in the fluid phase, however, and they drop out of solution.

The most common application of the GAS process is for the production of fine powders from hard-to-comminute materials such as explosives (Gallagher et al., 1989; Gallagher et al., 1992) and pharmaceuticals (Debenedetti, 1994; Chang et al., 1991; Chang and Randolph, 1990; Schmitt, 1994). The process ordinarily produces very fine particles with a narrow particle-size distribution, but other morphologies are possi-

---

Correspondence concerning this article should be addressed to R. M. Lemert.

ble. For example, nitroguanidine (an explosive used by the military) is typically obtained as long, needlelike crystals about 100 μm long by 5 μm wide. When it is precipitated from N,N-dimethylformamide (DMF) using chlorodifluoromethane, though, products ranging from uniform particles 5 μm in diameter to "starbursts" about 30 μm wide and "snowballs" about 300 μm wide are formed (Gallagher et al., 1992). A similar approach produces uniform insulin particles with a diameter of 2.0–2.5 μm that retain the biological activity of the source material (Debenedetti, 1994). Debenedetti (Debenedetti, 1994; Yeo et al., 1995) has also used the process to produce polyamide microfibers from DMSO and dimethyl acetamide (DMAC) solutions. Lithium chloride was required to solubilize the polymer in the DMAC, but Debenedetti found that it was possible to precipitate the polymer while keeping the salt in solution.

When several solutes are in solution the GAS process can be used as a type of fractional crystallization (Dixon and Johnston, 1991; Chang et al., 1994; Chang and Liou, 1993; Liou and Chang 1992). Debenedetti's work described in the previous paragraph, for example, takes advantage of this. The process has also been used to produce 90% pure anthracene from a 25% anthracene feed (Liou and Chang, 1992), to recover β-carotene from its oxidation products (Chang et al., 1991), and to produce a product enriched in trans-β-carotene from a mixture of isomers (Chang et al., 1994). The degree of separation that can be accomplished is a function of the relative supersaturation ratios of the different solutes (Chang et al., 1994; Chang and Liou, 1993).

The PCA process, which is a more recent development than the GAS process, has been used primarily to produce particles having selected morphologies. Johnston and coworkers, for example, have used the process to produce polymeric microspheres (Dixon et al., 1993, 1994), hollow microballoons (Dixon et al., 1993, 1994), and microfibers (Dixon and Johnston, 1993; Luna-Barcenas et al., 1995). The morphology produced by the process depends on whether the expansion path enters the spinodal decomposition zone and how fast the precipitation occurs (Dixon et al., 1993).

To date there has been no direct experimental study of the polarity of a liquid phase exposed to a supercritical fluid antisolvent. Dixon and Johnston (1991), however, have performed a theoretical analysis of the situation. They found that conventional Regular Solution Theory can describe the (relatively ideal) liquid phase at low pressures. At higher pressures an expanded liquid equation of state is necessary.

The objective of this study is to examine experimentally the effect of process conditions (pressure and temperature) on the polarity of the liquid phase in an antisolvent process. This will be accomplished using conventional solvatochromic techniques based on the behavior of Phenol Blue, a dye that is used as the basis for a commonly accepted scale of solvent polarity (Reichardt, 1979). The experimental results will be compared to predictions based on the bulk physical properties (dielectric constant and refractive index) of the liquid phase, which will allow us to comment on the microscopic structure of this phase. A comparison will also be made to results in the literature obtained from studies of single-phase mixtures at similar conditions. We will also examine the ability of the NRTL (nonrandom two liquid) model to predict the local composition of these highly asymmetric mixtures.

Experimental Procedures

The UV-visible spectra of Phenol Blue in the different solvent mixtures were obtained using a Varian Cary 5 spectrophotometer. Samples were contained in a custom stainless-steel cell, which is shown in Figure 1. The cell measures 6.35 cm wide by 6.35 cm deep by 11.8 cm high, and is fitted with sapphire windows 2.5 cm dia. by 1 cm thick. The cell is heated using up to six 50-W Chromalox cartridge heaters, and temperature control is provided by an Omega CN9000A controller fitted with a type K thermocouple. The power sent to the cartridge heaters was moderated using a Variac voltage regulator placed between the controller and the heaters. The pressure was adjusted using a High Pressure Equipment model 87-6-5 pressure generator and measured using a Sensotec model TJE/743-11 transducer and a model 060-3147-01 digital readout. A small Teflon-coated magnet inside the cell provides stirring to increase the rate at which the cell's contents reach equilibrium. The different components of the apparatus were connected to each other through 1/16 in. (1.6 mm) OD stainless-steel tubing. The apparatus is shown in Figure 2.

The unique feature of the cell shown in Figure 1 is the presence of two different chambers, the main sample chamber through which the light from the spectrophotometer passes and a vertical expansion chamber. The sample chamber has a diameter of 1.75 cm and a path length of 2.5 cm, giving it a volume of about 6.1 cm^3. The expansion chamber is 1.25 cm dia. by 5.1 cm long, giving an expansion volume of about 6.4 cm^3. It was designed to allow the liquid phase to expand as carbon dioxide dissolves in the solvent. The expansion volume is not visible from outside the cell, making the cell unsuitable for phase behavior studies. Any phases that form in this volume may not be detected. In this work, however, we are dealing only with mixtures for which the phase behavior is known, and the risk of having an unexpected phase present is minimal.

To obtain a spectrum, enough solvent was placed in the cell to substantially fill the main sample chamber. Sufficient Phenol Blue was then added to give an initial absorbance on

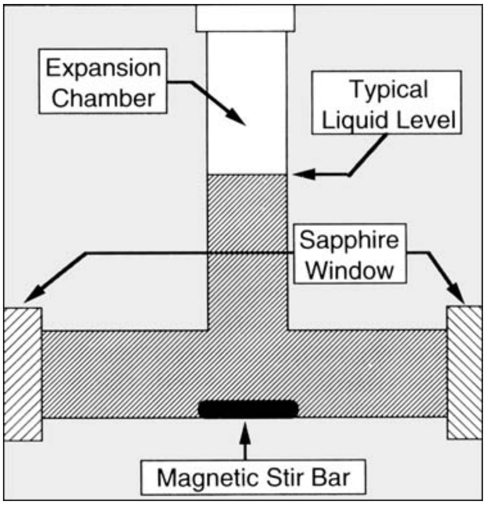

Figure 1. High-pressure cell for spectroscopic studies of gas antisolvent mixtures.

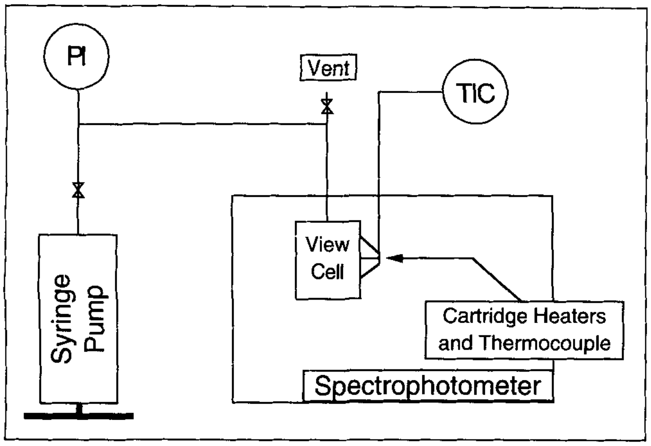

Figure 2. Apparatus used to perform the spectroscopic studies.

the order of three AU. The cell was sealed and heated to the desired temperature, and an initial CO_2-free spectrum was recorded. It was then flushed several times with CO_2 (raising the pressure to about 50 psia during each cycle) to remove residual air. Additional CO_2 was then added, and the cell's contents were mixed until equilibrium had been reached at the desired pressure. The resulting spectrum was then recorded, and the process was repeated at a new pressure. The location of the Phenol Blue peak (λ_{max}) was determined using the spectrophotometer's built-in peak find feature.

A potential problem during these experiments was the possibility that the expansion chamber might fill with the expanded liquid at some intermediate pressure. If this were to happen, further pressure increases would not produce a corresponding change in the liquid phase's composition. Since the expansion chamber is not visible during the experiments, care must be taken to watch for signs that this has occurred. For example, Phenol Blue's maximum absorbance should decrease with increasing pressure due to the expansion of the liquid phase that decreases the dye's molar concentration. If the liquid phase was no longer able to expand, further pressure increases would produce no corresponding change in the maximum absorption. Whenever this was observed, the experiment was terminated and a new one immediately begun. The new experiment was carried out using less solvent than was used in the original set of measurements, and the measurements commenced at an intermediate pressure where the results from the first run were felt to be valid. If the results of the second run agreed with those of the first, the data were considered to be representative of the equilibrium conditions. If the data from the second run disagreed with the earlier data but were consistent with the trends shown by the low-pressure data, the new data were considered more reliable and the earlier data were discarded.

The solvents used in the study (acetone, cyclohexane, methanol, THF, and toluene) were all reagent grade or better and used as received. Phenol Blue (*N,N*-dimethylindoaniline) was obtained from Aldrich and used as received. Its purity was checked by comparing its spectrum with values in the literature in different solvents. Instrument grade CO_2 was purchased from AGA Industrial Gases in Toledo, Ohio.

Results and Discussion

Experimental results

The results of our measurements of the location of the peak in the spectra of Phenol Blue (λ_{max}) in five different solvent–CO_2 mixtures are shown in Table 1. Each point represents the average of at least two (and usually three) separate scans. The reproducibility of λ_{max} is typically less than ± 0.3 nm. The data for the pure solvents are consistent with values reported earlier (Figueras, 1971; Kolling and Goodnight, 1973; Phillips and Brennecke, 1993), but differ slightly from the published values because of the higher temperatures used in this study. When the pure solvent measurements are repeated at 25°C, the data obtained are in complete agreement with the literature values.

In Figure 3, data for two of the systems (acetone–CO_2 and cyclohexane–CO_2, both at 35°C) are plotted as a function of pressure to illustrate the behavior observed in this study. As the pressure in the system increases, the polarity of the liquid phase decreases. This effect is small for cyclohexane, which is already a nonpolar solvent, but is much more significant for the other solvents. The rate at which the polarity changes with pressure is greater at pressures above about 40 bar than at lower pressures. This is consistent with the volumetric expansion behavior reported by Gallagher et al. (1989) and Dixon and Johnston (1991). Cyclohexanone increases its volume by about 15% as the CO_2 pressure is raised from ambient to ~ 70 bar, for example, but a further 15 bar increase in pressure causes an additional 250% volume increase (Gallagher et al., 1989).

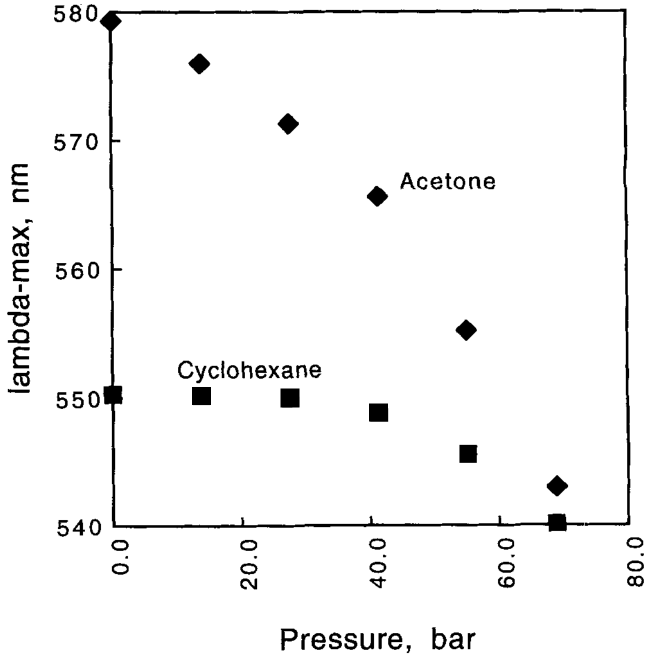

Figure 3. Experimentally observed solvatochromic shifts for the acetone-CO_2 (polar solvent) and cyclohexane-CO_2 (nonpolar solvent) systems showing the pressure effect on the polarity of the resulting solution.

The behavior shown is a result of the change in the composition of the liquid phase as the pressure increases.

The question arises as to whether the observed polarity changes are a direct result of the changing pressure of the system, or an indirect result of the changing density and/or composition of the liquid phase. We believe that the composition of the liquid phase is the controlling factor. The peak in Phenol Blue's spectrum used in this study arises from a $\pi-\pi^*$ transition in which the excited state has a dipole moment about 2.5 debye greater than the ground state (Reichert, 1979). Polar solvents are better able to stabilize this excited state (relative to the ground state) and therefore produce a red-shift in the dye's spectrum. This is reflected in Figure 3 by the fact that in pure acetone $\lambda_{\max}$ is about 580 nm, while in pure cyclohexane $\lambda_{\max}$ is about 550 nm. At higher pressures the liquid phase becomes rich in carbon dioxide (see below). Since carbon dioxide is very nonpolar, this significantly decreases the polarity of the resulting mixture. If a direct pressure effect was dominant, the polarity of the mixture would increase with increasing pressure (Kim and Johnston, 1987a). A density effect is not expected to be important because the density of the liquid phase is not expected to change significantly over the range of conditions being considered. It is interesting to note, however, that the two sets of data in Figure 3 seem to be approaching the same value of $\lambda_{\max}$ at high pressures. This occurs because the solutions are becoming very rich in CO_2, and as far as the dye is concerned the environments it finds itself in are becoming identical.

If the data for the THF and toluene solutions were included in Figure 3, they would lie between the two sets of data shown at all pressures. Interestingly, however, the data for these two solvents lie on essentially the same curve. This indicates that THF and toluene have essentially the same polarity at all pressures. The methanol data, on the other hand, gives a curve that is parallel to the acetone data but at wavelengths that are about 25 nm longer. Phenol Blue is known to be subject to specific interactions with alcohols, however, so this behavior is not unexpected (Kolling and Goodnight, 1973; Kim and Johnston, 1987a).

The acetone–CO_2 system has been examined in a previous study at similar conditions and over the same range of compositions (Kim and Johnston, 1987a). Their data were obtained at a constant pressure, however, and the composition was adjusted by mixing various amounts of the different components. In this study the composition was adjusted indirectly by changing the pressure. We have estimated the liquid phase compositions in our work using the Peng–Robinson equation of state (see the discussion below). In spite of the different techniques involved in the two studies, though, Figure 4 shows that our data are in excellent agreement with the earlier results. In other words, a change of pressure of up to 80 bar does not have a serious effect on the polarity of an incompressible liquid. (A pressure of 300 bar does produce a significant redshift, however [Kim and Johnston, 1987a].) This further supports our contention that the composition of the liquid phase governs the observed polarity behavior in these systems. Our data point at 6 mol % acetone (i.e., at a pressure of 69 bar) does not agree with the data of Kim and Johnston as well as the other data, but this most likely reflects a greater uncertainty in the estimated composition of the liquid phase.

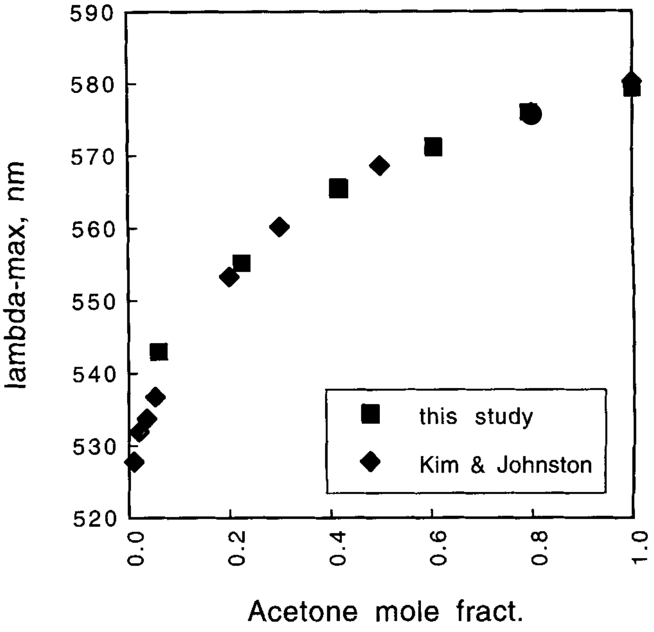

Figure 4. Data of this study obtained by increasing the pressure of the system with data of Kim and Johnston (1987a) at a constant pressure of 80 bar.

Both sets of data were obtained at 35°C.

Kim and Johnston also looked at the methanol–CO_2 system, but only at the CO_2-rich end of the phase diagram. A direct comparison of our data with their's would be difficult, but an approximate analysis suggests that there is a greater disagreement between the two studies for this system than was noted for the acetone–CO_2 system discussed previously, although the trend in the two studies is the same. At 80 bar, for instance, Kim and Johnston found that a solution containing 5.25 mol % methanol had a $\lambda_{\max}$ of 543.5 nm. In our study, we observed a $\lambda_{\max}$ of 578.8 nm at a pressure of 72 bar and an estimated methanol concentration of 4 mol %. In other words, we found that although our mixture was apparently more dilute in methanol, the Phenol Blue indicated that it was much more polar.

The reason for this discrepancy is not completely clear. One factor could be the relatively large uncertainty in the estimated composition of this solution since 72 bar is near the mixture critical pressure for this system at 35°C, and the Peng–Robinson equation often has problems giving accurate predictions at conditions near mixture critical points. However, extrapolating Kim and Johnston's data at 80 bar suggests that the minimum methanol content required to give our value of $\lambda_{\max}$ is about 15 mol % (assuming a straight-line extrapolation), and the actual value is likely to be higher since a plot of $\lambda_{\max}$ vs. methanol concentration is concave downward. Thus, this factor is expected to account for only a part of the discrepancy. The rest of the difference between our data and that of Kim and Johnston is thought to result from an unusually strong enhancement of the local composition in our work. Table 3 in Kim and Johnston shows that for a fixed bulk composition, the local solvent concentration about the dye increases significantly with decreasing pressure. At 300 bar, for example, the local methanol concentration is roughly three times the bulk concentration, whereas at 80 bar it's about seven times greater. Furthermore, the rate at which the local concentration increases is greater at lower pres-

Table 1. Estimated Compositions of the Liquid Phase for Various Solvent–Carbon Dioxide Mixtures Determined using the Peng–Robinson Equation of State and the λ_{max} Values Determined at these Conditions

Acetone (35°C)

Pres. bar	$x_{Acetone}$	λ_{max} nm
1.0	1.00	579.3
13.8	0.80	576.0
27.6	0.61	571.3
41.4	0.42	565.6
55.1	0.22	555.2
68.9	0.06	543.0

Acetone (55°C)

Pres. bar	$x_{Acetone}$	λ_{max} nm
3.4	0.96	569.8
6.9	0.92	569.7
13.8	0.85	569.7
17.2	0.81	572.0
20.7	0.78	571.6
24.1	0.74	571.0
27.6	0.71	569.7
34.5	0.64	568.8
41.4	0.57	567.6
55.1	0.43	562.6
68.9	0.30	557.3

Cyclohexane (35°C)

Pres. bar	x_{Cyclo}	λ_{max} nm
1.0	1.00	550.3
13.8	0.84	550.2
27.6	0.78	550.0
41.4	0.52	548.8
55.1	0.32	545.6
68.9	0.06	540.1

Methanol (35°C)

Pres. bar	x_{MeOH}	λ_{max} nm
1.0	1.00	606.4
10.3	0.90	603.4
20.7	0.80	602.5
31.0	0.69	599.7
41.4	0.56	596.5
51.7	0.42	593.5
62.0	0.22	588.4
72.4	0.04	578.8

Methanol (55°C)

Pres. bar	x_{MeOH}	λ_{max} nm
1.0	1.00	604.0
3.4	0.98	602.4
6.9	0.96	602.0
10.3	0.96	600.7
13.8	0.93	600.3
20.7	0.90	600.0
24.5	0.87	599.8
27.6	0.86	599.6
41.4	0.78	597.7
55.1	0.69	594.7
68.9	0.58	590.7

THF (35°C)

Pres. bar	x_{THF}	λ_{max} nm
1.0	1.00	569.8
13.8	0.82	569.8
27.6	0.64	565.6
41.4	0.46	559.2
55.1	0.26	549.5
68.9	0.06	537.6

Toluene (35°C)

Pres. bar	$x_{Toluene}$	λ_{max} nm
1.0	1.00	569.4
17.2	0.84	566.7
34.5	0.68	562.8
51.7	0.51	557.6
68.9	0.10	537.6

Toluene (55°C)

Pres. bar	$x_{Toluene}$	λ_{max} nm
1.0	1.00	566.5
13.8	0.90	566.2
27.6	0.80	565.2
41.4	0.70	562.4
55.1	0.61	559.0
68.9	0.47	554.8

sures. It seems reasonable that this trend would continue to 72 bar.

A more fundamental analysis of the data in Table 1 requires that the data be expressed in terms of a transition energy ($E_T = hc/\lambda_{max}$, where h is Planck's constant and c is the speed of light) and the composition of the solvent mixture. E_T were determined from the experimentally measured λ_{max}, while the Peng–Robinson equation of state (Peng and Robinson, 1976) was used to estimate the compositions. Binary interaction parameters in the equation of state were determined by fitting experimental VLE liquid-phase compositions for the acetone–CO_2 (Katayama et al., 1975), methanol–CO_2 (Katayama et al., 1975), toluene–CO_2 (Chang, 1992), and cyclohexane–CO_2 (Chang, 1992) systems. The estimated uncertainty in the composition of these mixtures is ±0.03 mole fraction except at the highest pressures, where the uncertainty may be as much as ±0.10 mole fraction. A value of 0.10 was assumed for the binary interaction parameter in the THF–CO_2 system, and therefore there is a greater uncertainty in the estimated compositions of this system. The parameters were assumed to be independent of temperature. The resulting plots are shown in Figures 5–7.

In each of the five systems investigated, similar behavior is observed. At low pressure the liquid phase contains very little CO_2 and the observed E_T is appropriate for the particular solvent. As the pressure increases the liquid phase becomes richer in CO_2, and E_T rises to show that the polarity of the liquid phase is decreasing. However, although the composition is typically a linear function of pressure (see Table 1), E_T is not a linear function of composition. In the solvent-rich mixtures E_T changes very little. In the CO_2-rich solutions, on the other hand, a significant influence of composition on E_T is observed. The upward concavity of the resulting curve is reported to indicate that the local environment around the dye molecule is enriched in the solvent compared to the bulk fluid (Kim and Johnston, 1987a).

In the acetone (Figure 5), methanol (Figure 6), and toluene (Figure 7) systems, data are shown for both 35 and 55°C. The data obtained at 55°C lies above the data at 35°C, indicating that mixtures having the same composition are less polar at higher temperatures. This reflects the decreased density of the mixtures at higher temperatures that reduces the mixture's cohesive energy density. The effect is not large, however, and can be considered secondary to the composition effect. Data could not be obtained for the acetone–carbon dioxide system at 55°C and one bar because the acetone tended to boil. There is also an apparent discontinuity in the 55°C acetone data at about 15 bar (~20 mol % CO_2). This discontinuity was reproducible, but we were unable to identify its cause.

In principle, the data in Figures 5–7 include an effect due to the pressure on the value of E_T in the system. As discussed earlier, however, this effect is small for an incompressible liquid at these conditions (Kim and Johnston, 1987a).

Predicted E_T values

Phenol Blue's solvatochromic behavior can be predicted from the solvent's bulk properties using a second order quantum mechanical perturbation theory. The resulting McRae equation, which relates the intrinsic solvent strength E_T^0 to the bulk dielectric constant ϵ and the bulk refractive index n, is shown as Eq. 1 (Kolling and Goodnight, 1973):

$$E_T^0 = A\left\{\frac{n^2-1}{2n^2+1}\right\} + B\left\{\frac{\epsilon-1}{\epsilon+2} - \frac{n^2-1}{n^2+2}\right\} + C. \quad (1)$$

The constants in Eq. 1 are properties of the dye and have the following values (Kolling and Goodnight, 1973): $A = -33.0$ kcal/mol; $B = -4.4$ kcal/mol; $C = 57.92$ kcal/mol. Equation

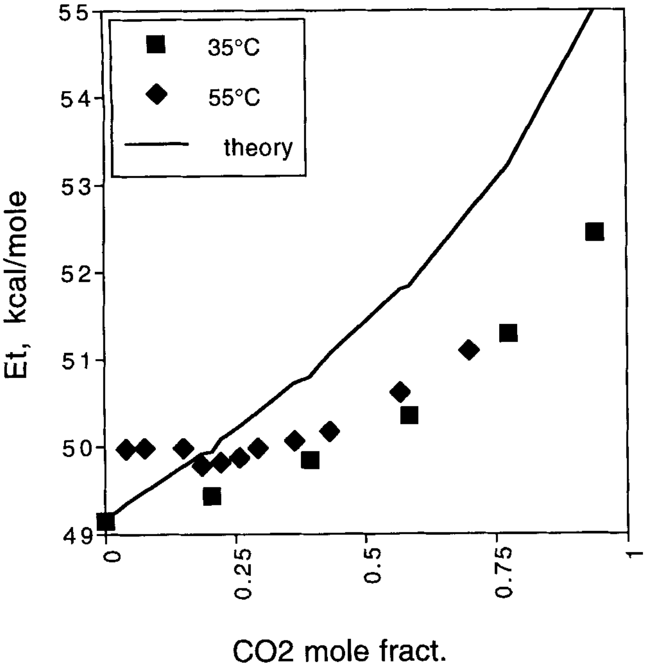

Figure 5. E_T for the acetone-carbon dioxide system.

The symbols represent the experimental data, and the solid line represents the predictions of the McRae equation (Eq. 1), which treats the solution as a homogeneous polarizable dielectric.

1 does not account for specific interactions such as hydrogen bonding. When specific interactions are important, the experimental value of E_T is separated into two terms, one arising from nonspecific forces and accounted for by Eq. 1, and the other arising from specific interactions (Kim and Johnston, 1987a). In other words,

$$E_T(\exp) = E_T^0 + E_T^S. \quad (2)$$

To use Eq. 1 two properties of the bulk mixture must be known; the mixture dielectric constant and the mixture refractive index. The mixture dielectric constant was estimated using the Kirkwood-Frölich equation (Böttcher, 1973; Böttcher and Bordewijk, 1978):

$$\frac{\epsilon-1}{12\pi\epsilon} = \frac{x_N(\epsilon_N-1)M_N}{4\pi(2\epsilon+\epsilon_N)\nu\rho_N} + \frac{x_P(\epsilon_P-1)M_P}{4\pi(2\epsilon+\epsilon_P)\nu\rho_P} + \frac{(2\epsilon+1)(\epsilon_P+2)^2 x_P N_A}{27kT(2\epsilon+\epsilon_P)^2\nu} g\mu^2, \quad (3)$$

where ν is the mixture molar volume; N_A is Avagadro's number; μ is the dipole moment of the polar component; and x_i, M_i, and ρ_i are the mole fraction, molecular weight, and density of the nonpolar (N) and polar (P) components, respectively. The contribution to the dielectric constant resulting from the molecular polarizability of each component is given by ϵ_i, which is determined using the Clausius-Mosotti equation:

$$\frac{\epsilon_i-1}{\epsilon_i+2} = \frac{4\pi N_A}{3\nu} x_i\alpha_i. \quad (4)$$

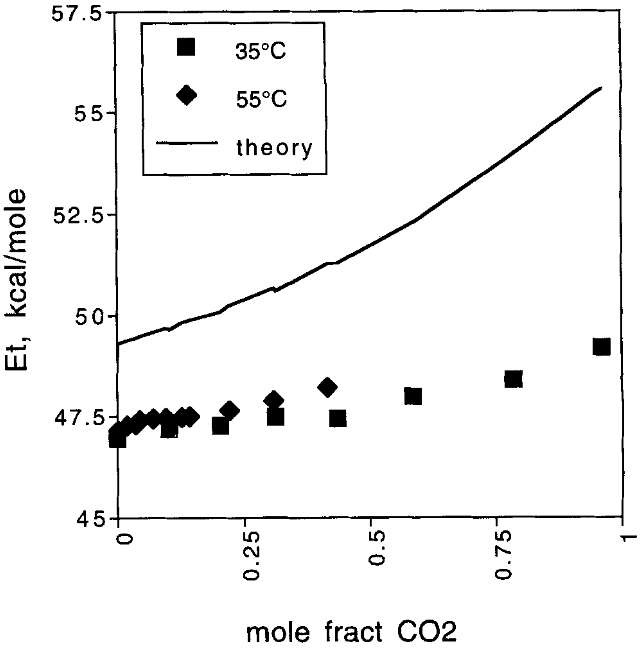

Figure 6. E_T for the methanol-carbon dioxide system.

The symbols represent the experimental data, and the solid line represents the predictions of the McRae equation (Eq. 1), which treats the solution as a homogeneous polarizable dielectric.

Application of Eq. 3 requires knowledge of the behavior of the Kirkwood structure correlation factor g as a function of the composition of the mixture. This factor accounts for nearest-neighbor dipole-dipole interactions, and $g = 1$ indicates freely rotating, noninteracting dipoles. Dombro et al. (1991) measured the dielectric constant of a series of

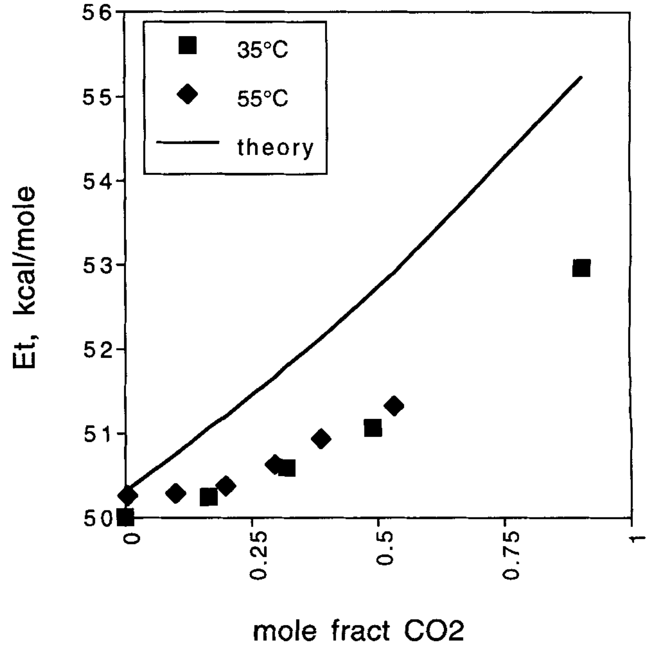

Figure 7. E_T for the toluene-carbon dioxide system.

The symbols represent the experimental data, and the solid line represents the predictions of the McRae equation (Eq. 1), which treats the solution as a homogeneous polarizable dielectric.

methanol–carbon dioxide mixtures at pressures to 240 bar and at temperatures ranging from 90 to 115°C. They then solved Eq. 3 for the Kirkwood structure factor using the experimental dielectric measurements. According to Figure 9 of Dombro et al., at a constant density, g is approximately a linear function of the composition of the mixture. We therefore make that assumption in this work. Since carbon dioxide does not have a dipole moment, we assume $g = 1$ in pure CO_2. The dielectric constant of the pure solvent at the temperature of interest is used to determine g for that component.

The refractive index of the different mixtures was estimated using the Lorentz–Lorenz relation (Schulte and Kauffman, 1994),

$$\frac{n^2-1}{n^2+2} = x_P\left(\frac{n_P^2-1}{n_P^2+2}\right) + x_N\left(\frac{n_N^2-1}{n_N^2+2}\right). \qquad (5)$$

Schulte and Kauffman included an empirical correction in Eq. 5 to account for the local structure of the solvent. Since Eq. 1 is intended to predict E_T in the absence of local solvent structure, however, we have neglected this correction.

Using the dielectric constants predicted by Eq. 3 and the refractive index values predicted by Eq. 5, Eq. 1 was used to predict E_T^0 for the five solvent–CO_2 mixtures considered in this study at a temperature of 35°C. The results of these calculations are shown in Figures 5–7 as solid lines. Except for methanol, the predicted and experimental E_T for the pure solvents are within 0.5 kcal/mol of each other. The experimental E_T of methanol is 1.95 kcal/mol less than the theoretical value. This is consistent with Kim and Johnston's (1987a) estimate of E_T^S for methanol of 1.6 kcal/mol, and can be attributed to the stabilization of the dye's excited state by the hydrogen bond donor character of methanol. At the other end of the composition scale, all five of the theoretical E_T curves extrapolate to a value of about 55.85 kcal/mole for pure carbon dioxide. This is also consistent with the experimental results of Kim and Johnston (1987a), which would suggest that a pressure of 65–70 bar is required to produce this value of E_T for Phenol Blue at 35°C. The maximum pressure in this study was 69 bar.

At intermediate compositions, the experimental E_T are significantly less than the values predicted by Eq. 1. This indicates that the dye is stabilized to a greater degree than can be accounted for by assuming that the solution is a homogeneous mixture, an assumption implicit in the use of Eq. 1. It has been shown that this extra stabilization is the result of an enrichment of the local environment about the dye molecules in the more polar component of the mixture (Kim and Johnston, 1987a,b; Phillips and Brennecke, 1993). In other words, the solution may contain 50 mol % toluene (for example) and would therefore be expected to produce an E_T of 52.75 kcal/mol. As far as the dye is concerned, however, it "sees" a solution that contains about 80 mol % toluene. In the remainder of this article, we will consider the local structures of these mixtures in greater detail.

Evaluation of local compositions

To estimate the local composition of the solvent environment about the dye, we assume that the observed transition energies (E_T) are the result of a linear combination of the transition energies due to each solvent. Following Phillips and Brennecke (1993) and Kim and Johnston (1987a), we assume that the residual transition energies have the following form:

$$\Delta E_T^m = x_{12}\Delta E_T^1 + x_{32}\Delta E_T^3, \qquad (6)$$

where component 1 is taken to be carbon dioxide, component 2 the dye, and component 3 the liquid solvent. The residual transition energy ΔE_T ($= E_T - E_T^{\text{ideal gas}}$) represents the stabilization produced by the solvent shell. The dye is assumed to be at infinite dilution so that solute–solute interactions can be ignored. We further assume that size effects due to the different solvents are negligible, so that Eq. 6 can be rewritten in terms of the measured E_T values as

$$E_T^m = x_{12}E_T^1 + x_{32}E_T^3. \qquad (7)$$

Phillips and Brennecke (1993) also assumed that the size effects were negligible. Kim and Johnston (1987a), on the other hand, accounted for this effect in their calculations. An examination of their data suggests that failure to account for the different molecular sizes introduces a relative error of about 10% in the estimated local compositions. This degree of accuracy is felt to be sufficient to allow at least a semiquantitative analysis.

In order to use Eq. 7 to estimate the local composition of the mixture, values of E_T^m, E_T^1, and E_T^3 are required. Values of E_T^m are taken directly from the experimental data at a given bulk composition, while values of E_T^3 are taken from the data for the pure solvents. To obtain a value of E_T^1 for carbon dioxide, we extrapolated the theoretical E_T^0 values in each system (shown by the solid lines in Figures 5–7) to the pure carbon dioxide limit and averaged the resulting values. This procedure gives an E_T for carbon dioxide of 55.85 kcal/mol. As noted earlier, a similar value can be obtained by extrapolating the experimental data of Kim and Johnston (1987a) to the same pressure (69 bar). Since the dye can be assumed to be at infinite dilution, x_{22} is taken to be zero, and x_{12} can therefore be replaced by $1 - x_{32}$.

In Figures 8 and 9 we plot the excess local compositions, defined as the difference between the local and the bulk concentrations of the solvent component in the mixture (i.e., $x_{32} - x_3$), as a function of x_3 for the acetone (Figure 8) and methanol (Figure 9) systems. The excess local composition in the acetone system is as high as 45 mol %, while the methanol system has excess local compositions of as much as 70 mol %. Plots of the data for the THF and toluene systems are similar to Figure 8, and the plot for the cyclohexane system is similar to Figure 9. Furthermore, all of the data are highly asymmetric, with maxima (when they occur) at very CO_2-rich conditions. In the acetone and THF systems, the maximum occurs at about 75 mol % CO_2, while the cyclohexane, methanol, and toluene systems give no indication of having passed through a maximum. Phillips and Brennecke (1993) showed similar asymmetries in their study of binary liquid mixtures, although the degree of asymmetry was substantially smaller. They also reported maximum excess local compositions on the order of 30 mol %, significantly lower than the values reported here.

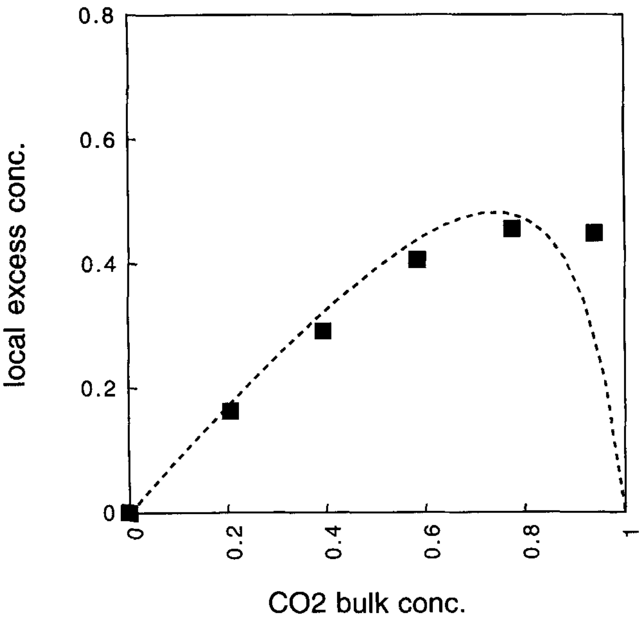

Figure 8. Excess local solvent mole fraction in the acetone-carbon dioxide system at 35°C as a function of the bulk composition of the fluid.

The dashed line represents the predictions of the NRTL equation.

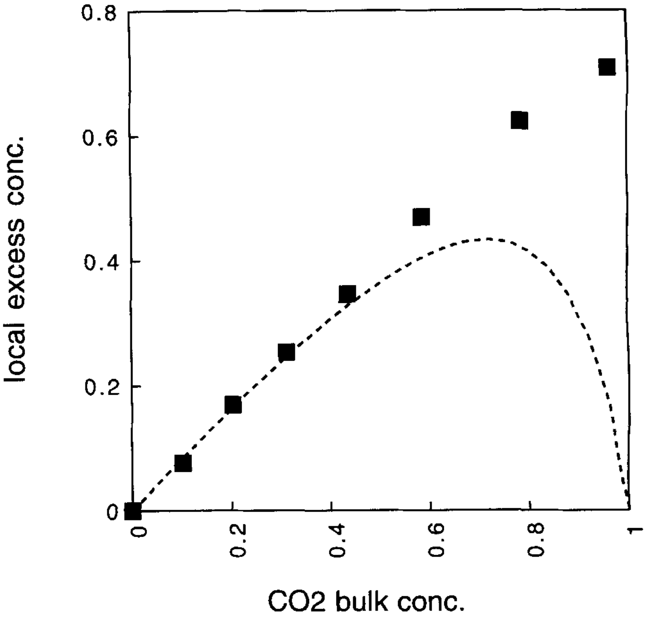

Figure 9. Excess local solvent mole fraction in the methanol-carbon dioxide system at 35°C as a function of the bulk composition of the fluid.

The dashed line represents the predictions of the NRTL equation.

The behavior of the acetone, THF, and toluene systems is not unreasonable. Certainly there is a large difference in the properties of these solvents and those of carbon dioxide, so a large asymmetry in the excess local compositions is to be expected. Furthermore, the polarities of toluene and THF (as indicated by Phenol Blue) are similar, and thus these solvents could be expected to give similar local composition behavior. One might expect acetone, which Phenol Blue indicates to be more polar than the other two solvents, to produce higher local concentrations than the other solvents. Phillips and Brennecke (1993) provide evidence that there is a weak specific interaction between Phenol Blue and toluene, however, and it would be reasonable if THF also underwent the same type of interaction. These interactions are apparently enough to offset the lower polarity of these solvents. Similarly, the known interactions between methanol and Phenol Blue (Kolling and Goodnight, 1973; Figueras, 1971; Kim and Johnston, 1987a) produce a significantly larger local composition enhancement for this system. At first glance the behavior of cyclohexane is fairly surprising. It has no permanent dipole moment or sites that could give specific interactions with Phenol Blue, and yet it gives local composition enhancements as large as those produced by methanol. It has a large polarizability, however, that is almost twice that of acetone and nearly four times that of methanol (Prausnitz et al., 1986). Thus, induction forces account for cyclohexane's unexpected behavior.

Another factor contributing to the asymmetry of the excess local compositions shown in Figures 8 and 9 is the relative compressibilities of the solvent-rich and CO_2-rich solutions being studied. The CO_2-rich solutions are similar to entrainer-doped supercritical fluids, and therefore are fairly compressible. As a result the local density enhancements in this study, and the resulting enhancements in the local composition, are greatest when the CO_2 concentrations are highest (Kim and Johnston, 1987b; Lemert and DeSimone, 1991). Note that this result is a consequence of the path being followed in this study. In general, the maximum local density enhancement in a supercritical fluid occurs at a bulk density one-third to one-half of the critical density (Sun et al., 1992; Knutson et al., 1992; Carlier and Randolph, 1993).

Phillips and Brennecke (1993) tested the ability of the NRTL equation (Renon and Prausnitz, 1968) to predict the local compositions about Phenol Blue in a series of binary liquid mixtures. They found that the predictions of the model were generally very accurate except for mixtures containing toluene. They attribute the poor predictions for toluene to specific interactions that increase Phenol Blue's solubility and produce an incorrect value for the binary interaction energy parameter (τ_{ij}). They selected this equation because it has been found relatively successful in describing liquid-liquid equilibrium, which they feel is a more stringent test of an excess Gibbs free-energy model than vapor-liquid equilibrium. Based on the success of Phillips and Brennecke, we have elected to apply the NRTL equation to our data.

The following expressions can be written for the local mole fractions about a molecule of Phenol Blue (component 2) in a ternary mixture;

$$x_{12} = \frac{x_1 \exp[-\alpha_{21}(\tau_{12} - \tau_{32})]}{x_3 + x_1 \exp[-\alpha_{21}(\tau_{12} - \tau_{32})]} \tag{8}$$

$$x_{22} = 0 \tag{9}$$

$$x_{32} = \frac{x_3 \exp[-\alpha_{23}(\tau_{32} - \tau_{12})]}{x_1 + x_3 \exp[-\alpha_{23}(\tau_{32} - \tau_{12})]}. \tag{10}$$

The nonrandomness factor α_{ij} is taken to be 0.3 following conventional practice (Prausnitz et al., 1986). Phenol Blue is assumed to be at infinite dilution, and its mole fraction is therefore taken to be negligible.

Application of Eqs. 8–10 requires knowledge both of the bulk composition of the mixture (available from the experimental data) and of the binary interaction energies τ_{ij}. The latter can be obtained from measurements of the solubility of Phenol Blue in the various pure solvents. The expression for binary solid–liquid equilibrium is (Prausnitz et al., 1986)

$$\ln \frac{1}{\gamma_2 x_2} = \frac{\Delta h^f}{R T_T}\left(\frac{T_T}{T} - 1\right), \tag{11}$$

where we are neglecting the terms involving differences in heat capacities. Replacing the triple point temperature (T_T) with the normal melting point ($T_M = 133°\text{C}$), and replacing the heat of fusion term ($\Delta h^f / T_T$) with the entropy of fusion ($\Delta s^f = 41.7$ J/mol·K [Phillips and Brennecke, 1993]) allows us to rewrite Eq. 11 as

$$\ln(\gamma_2 x_2) = \frac{\Delta s^f}{R}\left(\frac{T_M}{T} - 1\right). \tag{12}$$

Knowing Phenol Blue's solubility x_2 therefore allows us to determine its activity coefficient γ_2. Since Phenol Blue is effectively at infinite dilution, the solvent's activity coefficient γ_1 is one. With the activity coefficients known, the binary interaction energies can be determined from (Renon and Prausnitz, 1968)

$$\ln \gamma_1 = x_2^2 \left[\frac{\tau_{21} G_{21}^2}{(x_1 + x_2 G_{21})^2} + \frac{\tau_{12} G_{12}}{(x_2 + x_1 G_{12})^2} \right] \tag{13}$$

$$\ln \gamma_2 = x_2^2 \left[\frac{\tau_{12} G_{12}^2}{(x_2 + x_1 G_{12})^2} + \frac{\tau_{21} G_{21}}{(x_1 + x_2 G_{21})^2} \right], \tag{14}$$

where

$$G_{12} = \exp(-\alpha_{12} \tau_{12}) \tag{15}$$

$$G_{21} = \exp(-\alpha_{21} \tau_{21}). \tag{16}$$

Phenol Blue solubilities were measured in the various liquid solvents used in this study at 35°C by contacting the dye with excess solvent and stirring vigorously. The saturated liquid was diluted and analyzed by UV-vis spectrophotometry using an independently determined Beer's Law plot. The resulting values are listed in Table 2. The solubility in carbon dioxide was estimated by extrapolating Kim and Johnston's (1987a) solubility data to our final pressure of 69 bar. The extrapolation was carried out by plotting the log of Phenol Blue's solubility against carbon dioxide's density.

The local compositions predicted by the NRTL equation are shown in Figures 8 and 9 by the solid lines. Results for the other systems were similar to those shown. In every case the predictions are reasonable at low CO_2 concentrations but deviate significantly from the experimental data at high CO_2 concentrations. Dixon and Johnston (1991) observed similar behavior using Regular Solution Theory (RST) to model their systems. The large degree of asymmetry in the excess local compositions is also reflected in the NRTL predictions, with the peaks in the curves occurring at about 75 mol % CO_2.

Table 2. Phenol Blue Solubility in Various Solvents at 35°C

Solvent	Phenol Blue Solubility mol fraction	τ_{12}
CO_2	0.30×10^{-5}*	13.2
Acetone	4.1×10^{-3}	6.18
Cyclohexane	1.7×10^{-3}	6.96
Methanol	1.6×10^{-3}	7.01
THF	7.4×10^{-3}	5.74
Toluene	5.3×10^{-3}	5.98

*Estimated value at 69 bar, determined by extrapolating Kim and Johnston's (1987a) data.

Conclusions

We have presented the first direct experimental measurements of the effect of pressure on the polarity of the liquid phase in liquid–fluid gas antisolvent mixtures. Large changes in the polarity of conventional organic liquid solvents are produced using supercritical fluid carbon dioxide at relatively low pressures (< 70 bar). At high pressures, the polarities of the liquid phases approach a common value (equivalent to that produced by pure carbon dioxide at 70 bar), except in cases where specific interactions between the solvatochromic dye and the solvent are known to occur. These polarity changes result from the change in the liquid phase's composition with pressure.

The experimental data have been used to estimate the local compositions of the liquid phase and how they change with pressure. In every case the local environment about the solvatochromic dye is enriched in the polar (liquid) component compared to the bulk composition. Excess local composition plots are highly asymmetric, with local compositions richer in the polar (liquid) component even at very high CO_2 bulk concentrations. This local enrichment is the result of two complementary effects: the enrichment due to favorable molecular interactions between the solvent and the dye, and the additional enrichment that results from compressibility effects in the near-critical CO_2-rich solutions. The NRTL equation is able to predict the behavior of these systems at low pressure (solvent-rich conditions), but an expanded-liquid model would be required at higher pressures where the carbon dioxide concentration is greater.

Acknowledgments

The authors hereby wish to acknowledge the financial support of the University of Toledo's Chemical Engineering Department, the University of Toledo's Small Grants Fund, and the Ohio State Board of Regents. They also wish to thank Mr. Matthew Pitts and Mr. David L. Baerlin for assistance in performing many of the calculations in this study.

Literature Cited

Böttcher, C. J. F., *Theory of Electric Polarization*, Vol. I, Elsevier, Amsterdam (1973).

Böttcher, C. J. F., and P. Bordewijk, *Theory of Electric Polarization*, Vol. II, Elsevier, Amsterdam (1978).

Brennecke, J. F., and C. A. Eckert, "Phase Equilibria for Supercritical Fluid Process Design," *AIChE J.*, **35**, 1409 (1989).

Carlier, C., and T. W. Randolph, "Dense-Gas Solvent-Solute Clusters at Near-Infinite Dilution: EPR Spectroscopic Evidence," *AIChE J.*, **39**, 876 (1993).

Chang, C. J., "The Solubility of Carbon Dioxide in Organic Solvents at Elevated Pressures," *Fluid Phase Equil*, **74**, 235 (1992).

Chang, C. M. J., and Y. Liou, "Purification of Polycyclic Aromatic Compounds Using Salting-Out Separation in High-Pressure CO_2," *J. Chem. Eng. Japan*, **26**, 517 (1993).

Chang, C. M. J., Y. Liou, and W.-J. Lan, "Relative Supersaturation Ratio and Separation Factor in Crystallization with High-Pressure CO_2," *Can. J. Chem. Eng.*, **72**, 56 (1994).

Chang, C. J., and A. D. Randolph, "Solvent Expansion and Solute Solubility Predictions in Gas-Expanded Liquids," *AIChE J.*, **36**, 939 (1990).

Chang, C. J., A. D. Randolph, and N. E. Craft, "Separation of β-Carotene Mixtures Precipitated from Liquid Solvents with High Pressure CO_2," *Biotech. Prog.*, **7**, 275 (1991).

Debenedetti, P. G., "Supercritical Fluids as Particle Formation Media," *Supercritical Fluids: Fundamentals for Applications*, E. Kiran and J. M. H. Levelt Sengers, eds., Kluwer, Boston, p. 719 (1994).

Dixon, D. J., and K. P. Johnston, "Molecular Thermodynamics of Solubilities in Gas Anti-Solvent Crystallization," *AIChE J.*, **37**, 1441 (1991).

Dixon, D. J., and K. P. Johnston, "Formation of Microporous Polymer Fibers by Precipitation with a Compressed Fluid Antisolvent," *J. Appl. Poly. Sci.*, **50**, 1929 (1993).

Dixon, D. J., K. P. Johnston, and R. A. Bodmeier, "Polymeric Materials Formed by Precipitation with a Compressed Fluid Antisolvent," *AIChE J.*, **39**, 127 (1993).

Dixon, D. J., G. Luna-Barcenas, and K. P. Johnston, "Microcellular Microspheres and Microballoons by Precipitation with a Vapor-Liquid Compressed Fluid Antisolvent," *Polymer*, **35**, 3998 (1994).

Dobbs, J. M., J. M. Wong, R. J. Lahiere, and K. P. Johnston, "Modification of Supercritical Fluid Phase Behavior Using Polar Cosolvents," *Ind. Eng. Chem. Res.*, **26**, 56 (1987).

Dombro, R. A., M. A. McHugh, G. A. Prentice, and C. R. Westgate, "Dielectric Constant Behavior of Carbon Dioxide-Methanol Mixtures in the Mixture-Critical and Liquid-Phase Regions," *Fluid Phase Equil.*, **61**, 227 (1991).

Figueras, J. J., "Hydrogen Bonding, Solvent Polarity, and Visible Spectrum of Phenol Blue and its Derivatives," *J. Amer. Chem. Soc.*, **93**, 3255 (1971).

Gallagher, P. M., M. P. Coffey, V. J. Krukonis, and N. Klasutis, "Gas Antisolvent Recrystallization: New Process to Recrystallize Compounds Insoluble in Supercritical Fluids," *Supercritical Fluid Science and Technology*, K. P. Johnson and J. M. L. Penninger, eds., Amer. Chem. Soc. Symp. Ser., No. 406, p. 334 (1989).

Gallagher, P. M., M. P. Coffey, V. J. Krukonis, and W. W. Hillstrom, "Gas Anti-Solvent Recrystallization of RDX: Formation of Ultra-Fine Particles of a Difficult-to-Comminute Explosive," *J. Supercrit. Fluids*, **5**, 130 (1992).

Gupta, R. B., C. J. Han, and K. P. Johnston, "Recovery of Proteins and Amino Acids from Reverse Micelles by Dehydration with Molecular Sieves," *Biotech. Bioeng.*, **44**, 830 (1994).

Gurdial, G. S., and N. R. Foster, "Solubility of o-Hydroxybenzoic Acid in Supercritical Carbon Dioxide," *Ind. Eng. Chem. Res.*, **30**, 575 (1991).

Harrison, K., J. Goveas, K. P. Johnston, and E. A. O'Rear, "Water-in-Carbon Dioxide Microemulsions with a Fluorocarbon-Hydrocarbon Hybrid Surfactant," *Langmuir*, **10**, 3536 (1994).

Katayama, T., K. Ohgaki, G. Maekawa, M. Goto, and T. Nagano, "Isothermal Vapor-Liquid Equilibria of Acetone-Carbon Dioxide and Methanol-Carbon Dioxide Systems at High Pressures," *J. Chem. Eng. Japan*, **8**, 89 (1975).

Kim, S., and K. P. Johnston, "Clustering in Supercritical Fluid Mixtures," *AIChE J.*, **33**, 1603 (1987a).

Kim, S., and K. P. Johnston, "Molecular Interactions in Dilute Supercritical Fluid Solutions," *Ind. Eng. Chem. Res.*, **26**, 1206 (1987b).

Kiran, E., and J. M. H. Levelt Sengers, eds., *Supercritical Fluids: Fundamentals for Application*, Kluwer, Boston (1994).

Knutson, B. L., D. L. Tomasko, C. A. Eckert, P. G. Debenedetti, and A. A. Chialvo, "Local Density Augmentation in Supercritical Solutions," *Supercritical Fluids Technology: Theoretical and Applied Approaches in Analytical Chemistry*, F. V. Bright and M. E. P. McNally, eds., Amer. Chem. Soc. Symp. Ser, No. 488, p. 60 (1992).

Kolling, O. W., and J. L. Goodnight, "Phenol Blue as a Solvent Polarity Indicator for Binary Aprotic Solvents," *Anal. Chem.*, **45**, 160 (1973).

Krukonis, V. J., and R. T. Kurnik, "Solubility of Solid Aromatic Isomers in Carbon Dioxide," *J. Chem. Eng. Data*, **30**, 247 (1985).

Lemert, R. M., and J. M. DeSimone, "Solvatochromic Characterization of Near- and Supercritical Ethane, Propane, and Dimethyl Ether Using 9-(α-Perfluoroheptyl-β,β-Dicyanovinyl) Julolidine," *J. Supercrit. Fluids*, **4**, 186 (1991).

Lemert, R. M., and K. P. Johnston, "Chemical Complexation Agents for Enhanced Solubilities in Supercritical Fluid Carbon Dioxide," *Ind. Eng. Chem. Res.*, **30**, 1222 (1991).

Liou, Y., and C. M. J. Chang, "Separation of Anthracene from Crude Anthracene Using Gas Antisolvent Recrystallization," *Sep. Sci. Technol.*, **27**, 1277 (1992).

Luna-Barcenas, G., S. K. Kanakia, K. P. Johnston, and I. C. Sanchez, "Semi-Crystalline Microfibrils and Hollow Fibers by Precipitation with a Compressed Fluid Antisolvent," *Polymer*, **36**, 3173 (1995).

McHugh, M. A., and V. J. Krukonis, *Supercritical Fluid Extraction: Principles and Practice*, Butterworths, Stoneham, MA (1994).

Newman, D. A., T. A. Hoefling, R. R. Beitle, E. J. Beckman, and R. M. Enick, "Phase Behavior of Fluoroether-Functional Amphiphiles in Supercritical Carbon Dioxide," *J. Supercrit. Fluids*, **6**, 205 (1993).

Peng, D. Y., and D. B. Robinson, "A New Two Constant Equation of State," *Ind. Eng. Chem. Fundam.*, **15**, 59 (1976).

Phillips, D. J., and J. F. Brennecke, "Spectroscopic Measurement of Local Compositions in Binary Liquid Solvents and Comparison to the NRTL Equation," *Ind. Eng. Chem. Res.*, **32**, 943 (1993).

Prausnitz, J. M., R. N. Lichtenthaler, and E. G. de Azevedo, *Molecular Thermodynamics of Fluid Phase Equilibria*, 2nd ed., Prentice-Hall, Englewood Cliffs, NJ (1986).

Reichert, C., *Solvent Effects in Organic Chemistry*, Verlag Chemie, Weinheim, (1979).

Renon, H., and J. M. Prausnitz, "Local Compositions in Thermodynamic Excess Functions for Liquid Mixtures," *AIChE J.*, **14**, 135 (1968).

Savage, P. I., S. Gopalan, T. I. Mizan, C. J. Martino, and E. E. Brock, "Reactions at Supercritical Conditions: Applications and Fundamentals," *AIChE J.*, **41**, 1723 (1995).

Schmitt, W. J., "Preparation of Finely Divided Powders by Carrier Solvent Injection into a Supercritical or Near Critical Fluid," AIChE Meeting, San Francisco (Nov., 1994).

Schulte, R. D., and J. F. Kauffman, "Solvation in Mixed Supercritical Fluids: TICT Spectra of Bis(4,4'-aminophenyl) Sulfone in Ethanol/CO_2," *J. Phys. Chem.*, **98**, 8793 (1994).

Stahl, E., "Coupling of Extraction with Supercritical Gases and Thin-Layer Chromatography," *J. Chromatog.*, **142**, 15 (1977).

Stahl, E., K. W. Quirin, and H. K. Mangold, "Extraction and Fractionation of Complex Lipid Mixtures with Dense Carbon Dioxide on a Microscale," *Chem. Phys. Lipids*, **31**, 319 (1982).

Sun, Y.-P., M. A. Fox, and K. P. Johnston, "Spectroscopic Studies of p-(N,N-Dimethylamino) benzonitrile and Ethyl *p*-(N,N-Dimethylamino) Benzoate in Supercritical Trifluoromethane, Carbon Dioxide, and Ethane," *J. Amer. Chem. Soc.*, **114**, 1187 (1992).

Yeo, S.-D., P. G. Debenedetti, M. Radosz, R. Giesa, and H.-W. Schmidt, "Supercritical Antisolvent Process for a Series of Substituted Para-Linked Aromatic Polyimides," *Macromol.*, **28**, 1316 (1995).

Manuscript received Aug. 18, 1995, and revision received Oct. 30, 1995.